DOI: 10.1002/ejic.200700262

Mu-35: A Fluorogallophosphate Obtained by In Situ Generation of the Template

Louwanda Lakiss,[a] Angélique Simon-Masseron,*[a] Florence Porcher,[b] Séverinne Rigolet,[a] and Joël Patarin[a]

Keywords: Fluorine / Gallophosphate / Structure elucidation / Hydrothermal synthesis

A two-dimensional microporous fluorogallophosphate, named Mu-35, closely related to ULM-8, was hydrothermally synthesized by in situ generation of the structure-directing agent. The precursor of the structure-directing agent is ethylformamide, which is generated in situ by decomposition, and goes on to form ethylamine molecules that act as templates in the medium used for the synthesis. The fluorogallophosphate Mu-35 (Mu is Mulhouse), $Ga_3(PO_4)_2(HPO_4)F_3(C_2H_8N)_2$-$(C_2H_7N)_{0.5}$ (Z = 8), crystallizes in the orthorhombic space group *Pbcn* with the following unit cell parameters: a = 22.117(1), b = 17.3740(8), c = 10.1550(4) Å. The structure of fluorogallophosphate Mu-35 was determined from single-crystal XRD data. It exhibits anionic layers composed of an unusual arrangement of three-, five-, and eight-membered rings (MR) [Ga_2PO_2F, $Ga_3P_2O_4F$, and $Ga_3P_3O_8$, respectively], and intercalated by protonated and nonprotonated ethylamine molecules. Mu-35 was also characterized by powder XRD, SEM, elemental and thermal analyses, and solid-state NMR spectroscopy (^{1}H, ^{13}C, ^{19}F, and ^{31}P MAS and ^{1}H-^{31}P HETCOR experiments).

Introduction

In the last years, the search for new microporous materials has attracted special interest due to their potential uses as molecular sieves, heterogeneous catalysts, or ion exchangers.[1] After the discovery of the aluminophosphates by Wilson et al.,[2] research in the field of microporous phosphates was extended to different metals. The substitution of aluminium by other metals (Zn, Ga, etc.) has been reported. Among these materials, gallophosphates have attracted special attention; they allow a wide variety of structures to be formed owing to the gallium atoms, which can adopt four-, five-, and six-coordinations. Moreover the use of fluorine in the starting mixture enabled us to investigate new systems.[3] By introducing fluorine in the medium used for the synthesis, numerous fluorogallophosphates were obtained[4–5] such as cloverite, which is molecular sieves that contain a large 3D pore channel system.[6] In most cases, F^- was found to be present in the inorganic framework as terminal Ga–F groups, bridging gallium atoms, or trapped into small building units such as the so-called double four rings (D4R units). In this case, it seems that fluorine, besides its mineralizing role, plays a templating role and stabilizes these units.[5–8] A large number of metallophosphates with 0D, 1D, 2D, or 3D frameworks have been reported.[3–15] One way to obtain new materials is to exploit the in situ generation of the structure-directing agent. By this synthetic route, solvent or precursors of the templates are introduced into the starting mixtures, and during the synthesis, they partly decompose into molecules that act as templates. Few applications of such a synthetic technique have been reported; for instance, the in situ generation of structure-directing agents from 1,5-diaminopentane,[16] guanidinium cations,[17–19] piperazine,[20] dichloride of benzylviologen,[21] or urea derivatives.[22,23] In 1998, a new type of template precursor (i.e. alkylformamide molecules) was tested in the laboratory. Thus, it was possible to produce the two-layered aluminophosphates Mu-4[9] and Mu-7[10] and, more recently, the gallophosphates MIL30,[11] Mu-30,[12] Ea-TREN-GaPO,[13] Mu-33,[14] and Mu-34.[15]

In this paper, we report the synthesis, the structure determination, and the characterization of a new porous 2D fluorogallophosphate named Mu-35 that was obtained by using ethylformamide (EFD) as a precursor of ethylamine, which acts as the structure-directing agent (SDA).

Results and Discussion

Synthesis and Crystal Morphology

The results concerning the synthesis of fluorogallophosphate Mu-35 are summarized in Table 1. The fluoro-

[a] Laboratoire de Matériaux à Porosité Contrôlée, UMR CNRS 7016, Université de Haute Alsace, ENSCMu,
3 rue Alfred Werner, 68093 Mulhouse Cedex, France
Fax: +33-3-89336885
E-mail: Angelique.Simon-Masseron@uha.fr
[b] Laboratoire de Cristallographie et Modélisation des Matériaux Minéraux et Biologiques UMR CNRS 7036, Faculté des Sciences, Université Henri Poincaré Nancy 1,
B. P. 239, 54506 Vandoeuvre-lès-Nancy Cedex, France
Supporting information for this article is available on the WWW under http://www.eurjic.org or from the author.

Table 1. Syntheses performed in the system $GaOOH/H_3PO_4/HF/ethylformamide$ (EFD)/tripropylamine (TPA)/H_2O.

Sample (Heating time, d)	Molar composition of the starting mixture							XRD results
	GaOOH	H_3PO_4	HF	EFD	H_2O	TPA	T [°C]	
A (7)	1	2	2	6	5.8[a]	–	170	Mu-35
B (7)	1	2	–	6	5.8[a]	–	170	$GaPO_4$-C_4
C (7)	1	2	2	6	5.8[a]	–	200	Phase A + impurity[b]
D (4)	1	2	2	6	5.8[a]	–	130	Phase B[c]
E (4)	2	2	2	2	80	–	170	Quartz
F (4)	2	2	2	2	16.3	1	170	Mu-35[d]

[a] H_2O arising from orthophosphoric (85% H_3PO_4) and hydrofluoric acid (40% HF). [b] Unknown phase. [c] Structure in progress. [d] Impurity eliminated by ultrasound.

gallophosphate Mu-35 was first prepared as white powder in a fluorine quasinonaqueous medium with a Ga/P molar ratio equal to 0.5 (sample A). The presence of fluorine is crucial as the $GaPO_4$-C_4[24] crystallizes when fluorine is not present in the mixture (sample B). A change in the heating temperature (samples A, C, and D) influences the nature of the crystallized phase. For a similar starting molar composition, but with a higher heating temperature (200 °C, sample C), a nonidentified phase (phase A) with traces of an impurity crystallizes. Moreover, for a lower heating temperature (130 °C, sample D), another phase, namely phase B, was obtained. Experiments were also performed in aqueous medium. In a diluted medium (sample E, 80 H_2O) a quartz-type gallophosphate was obtained, whereas in a more concentrated medium (sample F, 16.3 H_2O) large crystals of Mu-35 suitable for single crystal XRD determination were formed.

As shown in Figure 1, the crystals of the fluorogallophosphate Mu-35-sample A and Mu-35-sample F display rectangular shapes, with average sizes of 150×20 and 150×30 μm^2, respectively.

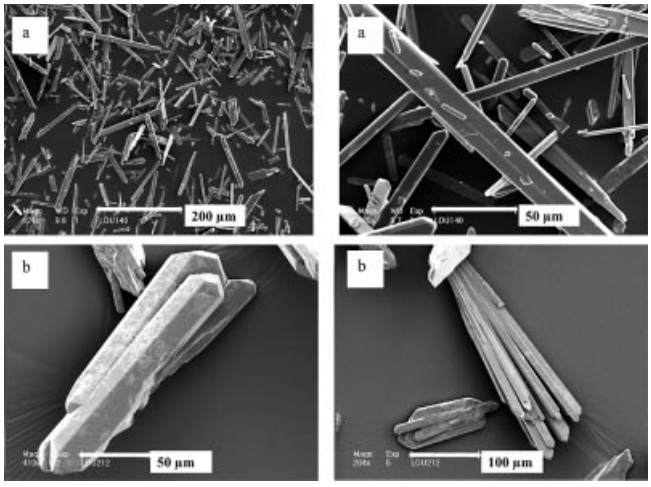

Figure 1. Scanning electron micrographs of (a) the fluorogallophosphate Mu-35-sample A, (b) the fluorogallophosphate Mu-35-sample F.

XRD Analysis

The experimental powder diffraction pattern of the fluorogallophosphate Mu-35 is reported in Figure 2a. It was indexed in orthorhombic symmetry with the following unit cell parameters: a = 22.410(3), b = 17.478(3), c = 10.2060(18) Å. For comparison, the simulated XRD pattern of Mu-35 is reported in Figure 2b.

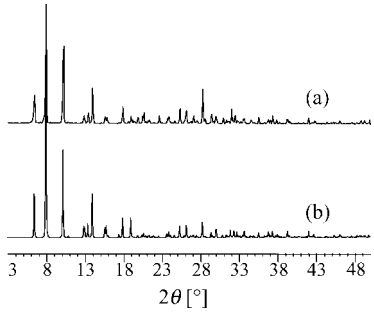

Figure 2. XRD patterns of the fluorogallophosphate Mu-35: (a) experimental pattern, (b) simulated pattern (radiation Cu-$K_{\alpha 1}$).

Chemical and Thermal Analyses

According to elemental analyses, the as-synthesized Mu-35 sample has the following composition: Ga 30, P 15, F 8, N 5, C 9 wt.-%. Such results are in agreement with the composition obtained from the structure determined: Ga 31, P 14, F 8, N 5, C 9 wt.-%. The experimental C/N molar ratio equal to 2 is different from the value expected for ethylformamide (3C:1N), which proves that the solvent partly decomposes into ethylamine (EA) (3C:1N) during the synthesis. This was later confirmed by ^{13}C NMR spectroscopy (see below). As previously shown for other phosphate-based materials synthesized in the presence of alkylformamide,[9–15] the in situ release of the corresponding protonated amine during the synthesis appears to be a key step in the crystallization of this lamellar fluorogallophosphate. Indeed, experiments using ethylamine directly introduced in the starting mixture led to the crystallization of a quartz-type gallophosphate.

The thermal behavior of the fluorogallophosphate Mu-35 was investigated by TG/DTA thermal analyses. The TG and DTA curves of the as-synthesized material are reported in Figure 3. The total weight loss occurs mainly in two steps. A small weight loss close to 3 wt.-% appears before 250 °C. It might correspond to the removal of water molecules physisorbed and arise from the dehydroxylation reaction. The main weight loss (18.3 wt.-%) occurs between 250

and 500 °C. It is associated with endothermic components on the DTA curve, and can be attributed to desorption and decomposition of the ethylamine molecules and to the removal of the fluorine atoms (probably under the form of HF). After heating at 800 °C, the XRD analysis of the residue shows that the starting material was transformed by an amorphization–recrystallization process into a cristobalite-type gallophosphate.

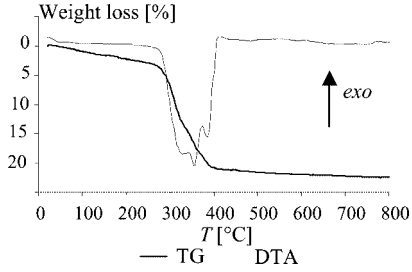

Figure 3. Thermal analyses (TG and DTA) under air of the fluorogallophosphate Mu-35.

Structure Description

The structure of the fluorogallophosphate Mu-35 displays macroanionic layers composed of an arrangement of 3, 5, and 8 MR [Ga_2PO_2F, $Ga_3P_2O_4F$, and $Ga_4P_4O_8$, respectively]. These layers can be observed as the results of the condensation of fluorogallophosphate zig–zag chains (AAA) connected together along the *b* axis by the O5 oxygen atom (Figure 4). These zig–zag chains are built up from GaO_4F, GaO_3F_2, and GaO_4F_2 polyhedra linked by PO_4 tetrahedra. The asymmetric unit, reported in Figure 5, contains three crystallographically distinct Ga sites, two in fivefold coordination (Ga2 and Ga3) and one in sixfold coordination (Ga1). The structure also contains three crystallographically distinct P sites: the P1 and P2 sites share all their oxygen atoms with gallium neighbors, whereas P3 displays a hydroxy group O12, which points towards the layers. It should be noted that this oxygen atom, in addition to others (O1, O2, and O8), interact strongly with ethylamine molecules that are located between the layers through hydrogen bonds (‹N1–H1b···O1› = 1.92, N2–H2b···O2 = 2.02, ‹N2–H2c···O8› = 1.91, ‹N1–H1c···O12› = 1.85 Å). The structure could also be described as an arrangement of hexameric units (Ga_3P_3). These hexameric units are common in fluorinated gallium phosphates, as it has been observed in many 2D and 3D structures (ULM-8,[25] MIL-30,[11] MIL-50[26]). These units are joined together by two opposite orientations, which then generates the pseudo-membered rings described below. It is noteworthy that the structure of the Mu-35 is closely related to that of the fluorogallophosphate ULM-8.[25] Indeed, in comparison to the ULM-8 compound, the hexameric unit here possesses three fluorine ions instead of the usual two, and one hydroxy group P–OH. Furthermore, in our compound the sheets are shifted by a factor of *b*/2. Such a displacement could be a key factor for the transformation of the 2D Mu-35 compound into the 3D TREN-GaPO phase. To confirm this hypothesis, experimental study of the 2D Mu-35/3-D TREN-GaPO transformation, by hydrothermal treatment, is in progress.

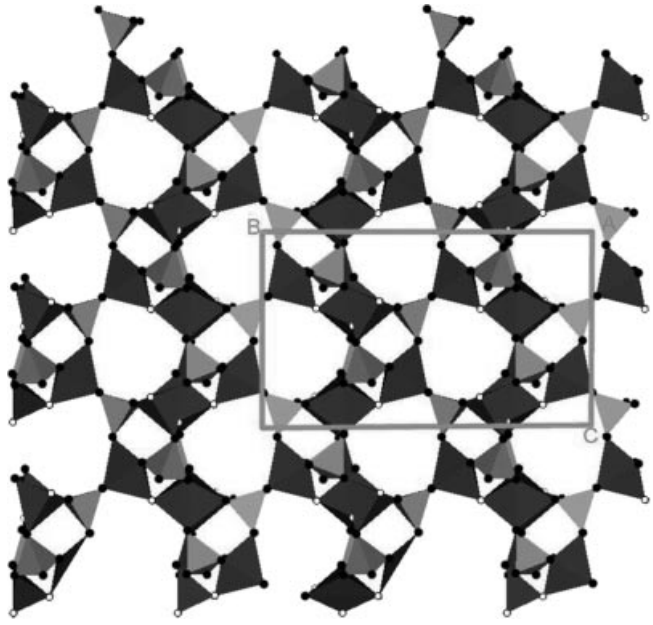

Figure 4. Projection of the structure of the fluorogallophosphate Mu-35 along the *a* axis, which shows the inorganic chains connected by O5 with 8-MR openings. Black spheres: O, open circles: F, dark grey polyhedra: Ga, light grey polyhedra: P.

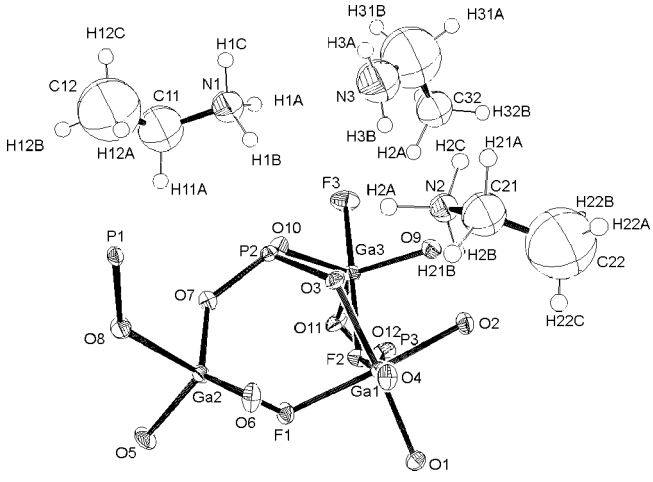

Figure 5. The asymmetric building unit of the fluorogallophosphate Mu-35.

The fluorine atoms are located on three nonequivalent crystallographic sites: two correspond to bridging species F1 and F2, which interact with the ethylamine molecules through hydrogen bonds [‹N2–H2a···F2› = 2.06(4), ‹N2–H2a···F1› = 2.22(4) Å; Table 2]. The third one (F3), which is connected to Ga3, is observed in the terminal position. The average ‹Ga–F› bond length is in good agreement with those reported for fluorogallophosphates.[15]

Table 2. Ethylamine-framework contacts with d(D···A) < 3.40 Å, d(H···A) < 2.33 Å, D–H···A > 100.0°. H···A distances and D–H···A angles are indicative only (H atoms fixed at their standard positions).

Donor	H	Acceptor	D–H	H···A	D···A	D–H···A
N1	H1A	F3	1.03(4)	1.80(4)	2.729(8)	149(4)
N1	H1B	O1	1.03(4)	1.92(4)	2.839(8)	147(4)
N1	H1B	O10	1.03(4)	2.30(4)	3.1071(8)	134(4)
N1	H1C	O12	1.03(3)	1.85(4)	2.861(8)	168(4)
N2	H2A	F1	1.02(3)	2.22(4)	2.835(7)	117(2)
N2	H2A	F2	1.02(3)	2.06(4)	3.049(7)	160(2)
N2	H2B	O2	1.02(2)	2.02(3)	3.029(7)	168(2)
N2	H2C	O8	1.03(3)	1.91(3)	2.887(7)	158(3)
C32	H32A	F3	1.04(8)	1.85(9)	2.74(2)	142(1)
C32	H32B	O6	1.02(9)	2.26(9)	3.10(2)	138(5)

To compensate for the negative charges of the framework, two of the three ethylamine molecules that are intercalated between the layers (N1 and N2, 8 × 2 molecules), are protonated. These molecules, which occupy a general position, are located inside the pseudo 12-membered ring (Figure 6). The remaining ethylamine molecule, which occupies the special N3 position, has an occupancy factor of 0.5, and it is nonprotonated and localized in the pseudo 8 MR.

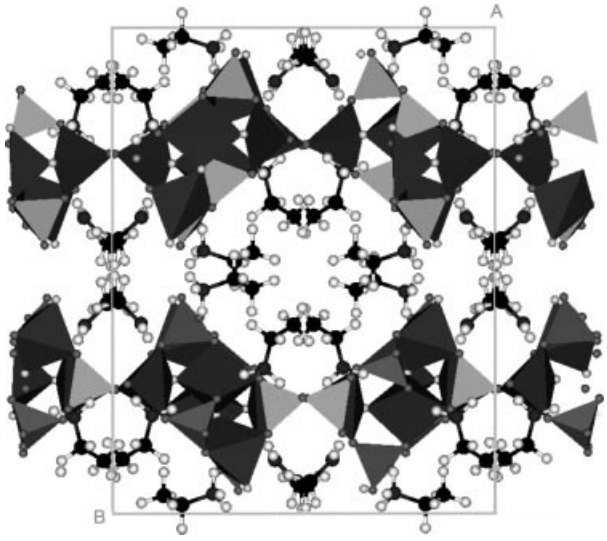

Figure 6. Projection of the structure of the fluorogallophosphate Mu-35 along the *c* axis, which shows the localization of the amine (black spheres). For a colored version of this figure see the Supporting Information.

^{13}C CP MAS NMR Spectroscopy

Figure 7 shows the proton decoupled ^{13}C MAS NMR spectrum of the fluorogallophosphate Mu-35. It displays two main signals located at ca. 13.1 and 35.2 ppm, which can be assigned to the CH_3 and CH_2 groups of the ethylamine molecules, respectively.[27] No carbonyl group is observed in this spectrum (resonance expected at about 160 ppm), which means that EFD is partly decomposed into ethylamine (EA) under our experimental conditions. The signal at δ = 13.1 ppm, which has a shoulder at δ = 14.1 ppm, can be attributed to the methyl groups of the ethylamine molecules. According to the ^{13}C isotropic chemical shifts (δ) known from liquid-state ^{13}C NMR [$\delta(CH_3)$ protonated molecules: 12.5 ppm and $\delta(CH_3)$ nonprotonated molecules: 19 ppm], these two signals could be assigned to the CH_3 groups of protonated and nonprotonated EA, respectively. Such a result confirms with agreement with the structure determination: the hypothesis of amine protonation. Indeed the relative areas of the two signals are close to 4 (δ = 13.1 ppm):1 (δ = 14.1 ppm).

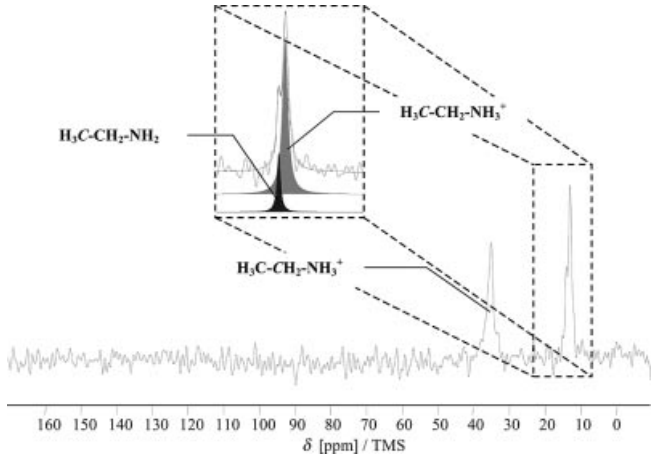

Figure 7. ^{1}H decoupled ^{13}C MAS spectrum of the fluorogallophosphate Mu-35 and its decomposition.

^{19}F MAS NMR Spectroscopy

As shown in the Figure 8, the ^{19}F MAS NMR spectrum of the as-synthesized product exhibits two signals located at –106.2 and –140.2 ppm. After decomposition, the relative areas are close to 2:1, respectively, indicating, in agreement with the structure determination, the existence of three crystallographically distinct fluorine sites. As observed for other fluorogallophosphates,[28–30] these signals could be assigned to the bridging fluorine species F1 and F2 and to the terminal fluorine species F3, respectively.

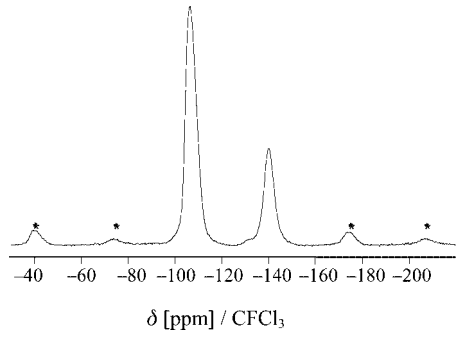

Figure 8. ^{19}F MAS NMR spectrum of the fluorogallophosphate Mu-35. * Spinning side bands.

^{1}H, ^{31}P and ^{1}H-^{31}P HETCOR NMR Spectroscopy

The ^{31}P MAS NMR spectrum of the fluorogallophosphate Mu-35, reported in Figure 9, displays three main signals at –3.4, –7, and –13.8 ppm. The relative areas are close to 1:1:1, which confirms, in agreement with the structure determination, the existence of three distinct crystallographic phosphorus sites. The decomposition shows that the signal at –7 ppm could be decomposed into two components (–6.2 and –7.2 ppm). It was noted that the intensity areas ratio between these two components varies with the amount of physisorbed water. This means that at the local order, the symmetry is probably lower, and the P3 phosphorus site splits into two different crystallographic sites.

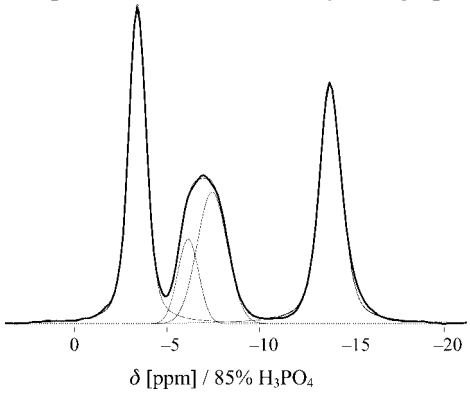

Figure 9. ^{31}P MAS NMR spectrum of the fluorogallophosphate Mu-35 and its decomposition.

The ^{1}H MAS NMR spectrum reported in Figure 10, displays at least four resonances at ca. 1.4, 3.4, 7.4, and 15.1 ppm. The resonances at δ = 1.4 and 3.4 ppm could be attributed to the CH_3 and CH_2 groups of the ethylamine molecules. According to the ^{1}H liquid-state NMR spectroscopic data, the signal located at 7.4 ppm could be assigned to the NH_3^+ and NH_2 groups. It is noteworthy that protons of NH_2 groups might be shielded because of the existence of hydrogen bonds with the oxygen atoms of physisorbed water molecules, which is expected to be observed at 4.7 ppm. The remaining signal at ca. 15.1 ppm could be assigned to the proton of the hydroxy group bound to the phosphorus atom (P–OH) that is in strong interaction with a water molecule through a hydrogen bond.

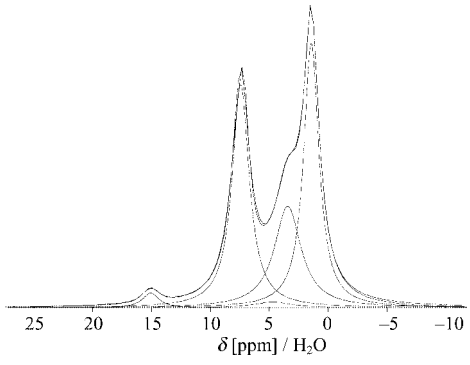

Figure 10. ^{1}H MAS NMR spectrum of the fluorogallophosphate Mu-35 and its decomposition.

A ^{1}H-^{31}P CP MAS NMR experiment was performed (spectrum not reported) to reveal the presence of the hydroxy group. For a contact time of 0.1 ms, an increase in the signal located at –7.0 ppm (Figure 9) was observed between the MAS and CP MAS spectra, which means, in agreement with the structure determination, that the corresponding phosphorus site is close to the proton and could be considered as a P–OH group. In Mu-35, this site could be assigned to P3.

To assign the different phosphorus signals, a 2D ^{1}H-^{31}P HETCOR experiment was performed. The 2D spectrum, shown in Figure 11, displays three signals for the P atoms located at –3.4, –7.0, and –13.8 ppm, which are characteristic of P*i*-H*j* interaction. It should be noted that only the phosphorus site associated to δ = –7.0 ppm has a strong interaction with the proton signal at ca. 15.1 ppm. Such a result confirms the assignment of the signal at –7.0 ppm to the phosphorus crystallographic P3 site. Unfortunately, it was not possible to clearly discriminate between P2 and P1.

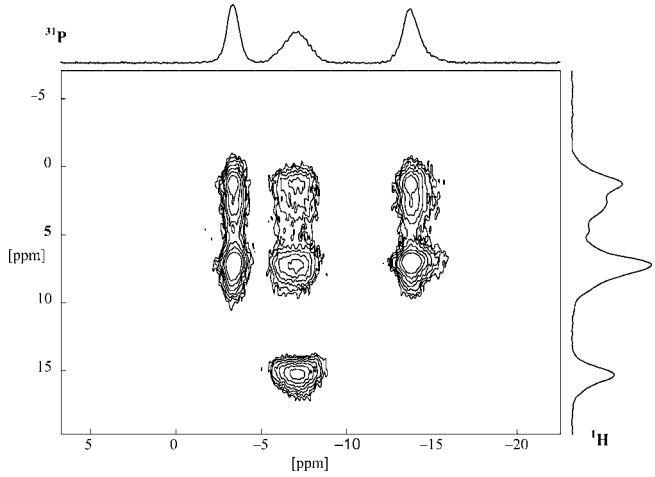

Figure 11. ^{1}H-^{31}P 2D HETCOR spectrum of the fluorogallophosphate Mu-35.

Conclusion

In this paper the synthesis and the characterization of a fluorogallophosphate Mu-35, with a rather unusual structure, was reported. It was prepared in an aqueous medium by using ethylformamide as the precursor of the structure-directing agent. As in several similar syntheses, ethylformamide decomposes during the synthesis, and the corresponding amine is found occluded in the final structure. The in situ release of the amine during the synthesis appears to be a key step in the crystallization of this lamellar fluorogallophosphate. Indeed, experiments using ethylamine directly in the starting mixture did not lead to the crystallization of this material.

The fluorogallophosphate Mu-35 displays anionic layers closely related to ULM-8, built from three-, five- and eight-membered rings. To compensate for the negative charges of the anionic layers, the ethylamine molecules that are located inside the pseudo 12 MR are protonated, which is in contrast to the ones observed inside the pseudo 8 MR.

Experimental Section

General: The fluorogallophosphate Mu-35 was prepared in an aqueous fluoride medium at 170 °C from a mixture containing ethylformamide as a precursor of the SDA (ethylamine). The molar composition of the starting mixture was 2 GaOOH/2 H_3PO_4/2 HF/2 ethylformamide (EFD)/16 H_2O. The water amount arises from the phosphorus and the fluoride sources. The pH value of the reaction mixture was adjusted to 2.5 with tripropylamine (TPA, Fluka 98 wt.-%), the latter presenting no structure-directing effect in the fluorine-containing gallophosphate system.[31] The amorphous gallium oxyhydroxide GaOOH was prepared by heating a gallium nitrate aqueous solution at 250 °C for 24 h. The other reactants were orthophosphoric acid (Labosi 85 wt.-%), hydrofluoric acid (Prolabo 40 wt.-%), and ethylformamide (EFD, Fluka 99 wt.-%).

Synthesis: The starting mixture was prepared by adding the amorphous gallium source (0.45 g) to water (0.36 g) under magnetic stirring. Then, ethylformamide (0.29 g), orthophosphoric acid (0.46 g), and hydrofluoric acid (0.2 g) were introduced. To increase the pH value of the solution to 2.5, tripropylamine (0.29 g) was added, and the mixture was stirred until homogeneous. Then, it was transferred to a 20-mL PTFE-lined stainless-steel autoclave and heated at 170 °C for 4 d. The product was filtered, washed with distilled water, and dried at 60 °C overnight.

Characterization: The as-synthesized product was characterized by powder X-ray diffraction (XRD) with a STOE STADI-P diffractometer equipped with a curved germanium (111) primary monochromator and a linear position-sensitive detector using Cu-$K_\alpha 1$ radiation (λ = 1.5406 Å). The morphology and average size of the crystals were determined by scanning electron microscopy (SEM) with a Philips XL30 microscope. Elemental analyses were performed with an induced coupled plasma technique by using atomic energy spectroscopy (ICP AES) for Ga and P, and by coulometric and catharometric methods for C and N quantifications, respectively. Thermogravimetric (TGA) and differential thermal (DTA) analyses were performed under air with a Setaram Labsys thermoanalyser with a heating rate of 5 °C min^{-1} up to 1000 °C. Solid-state NMR experiments were performed at r.t. with a Bruker DSX 400 spectrometer operating at B_0 = 9.4 T and a Bruker double channel high-speed 2.5 mm probe. The recording conditions are reported in Table 3. As the typical T_1 values measured for our sample by using inversion recovery was slightly less than 0.6 and 2.8 s for the ^{1}H and ^{19}F, respectively, the corresponding recycle delays were fixed to 3 and 15 s, respectively. Furthermore the ^{31}P spin lattice relaxation times (T_1) was measured with the saturation-recovery pulse sequence and it was found to be less than 68 s. Decompositions of the spectra were performed with WINFIT programs.[32]

Table 3. Recording conditions of the NMR spectra.

	^{1}H MAS	^{1}H decoupled ^{13}C MAS	^{31}P MAS	^{1}H-^{31}P CP MAS	^{1}H-^{31}P HETCOR	^{19}F MAS
Chemical shift reference	TMS	TMS	85% H_3PO_4	85% H_3PO_4	85% H_3PO_4	$CFCl_3$
Frequency [MHz]	400.2	100.6	161.98	161.98	161.98	376.5
Pulse width [μs]	5.5	2.5	3.5	4.5	4	4
Flip angle	π/2	π/4	π/2	π/2	π/2	π/2
Contact time [ms]	–	–	–	0.05–0.1	0.05	–
Recycle time [s]	3	60	30	10	3	20
Spinning rate [Hz]	25000	5000	25000	25000	25000	25000
Number of scans	8	832	64	64	200	32

Table 4. Experimental single-crystal XRD data and structure analysis of the fluorogallophosphate Mu-35.

Compound name	Mu-35
Chemical formula (asymmetric unit)	$[Ga_3(HPO_4)\ (PO_4)_2F_3(C_2H_8N)_{2.0}(C_2H_7N)_{0.5}]$
Cell parameters	a = 22.1170(11), b = 17.3740(8), c = 10.1550(4) Å α = 90°, β = 90°, γ = 90°
V [Å^3]	3902.2(3)
Space group, Z	*Pbcn*, 8
Density (calculated)	2.336(5)
Crystal size [μm]	170 × 90 × 50
Diffractometer	Oxford diffraction Xcalibur 2 + Sapphire CCD
Radiation source, Wavelength	Mo($K\alpha$) λ = 0.71073 Å
Absorption coefficient [mm^{-1}]	4.45
Transmission T_{min}/T_{max}	0.53/0.85
Temperature [K]	293
Reflections measured, independent	58820, 10701
Unique reflections Observed [$I > 3\sigma(I)$]	4642
Overall completeness ($sin\theta/\lambda_{max}$ = 0.88 Å^{-1})	90%
Internal agreement R_{int}[a]	0.078
Agreement factors after structural refinement [$I > 3\sigma(I)$]	R = 0.054, Rw = 0.058, goof = 2.53

[a]

$$R = \left(\sum_H \left\| F_{obs.} \right| - \left| kF_{calc.} \right\| \right) \Big/ \left(\sum_H \left| F_{obs.} \right| \right), \quad Rw = \left\{ \left(\sum_H w\left(\left| F_{obs.} \right| - \left| kF_{calc.} \right| \right)^2 \right) \Big/ \left(\sum_H w \left| F_{obs.} \right|^2 \right) \right\}^{1/2}$$

$$Goof = \left\{ \left(\sum_H w\left(\left| F_{obs.} \right| - \left| kF_{calc.} \right| \right)^2 \right) \Big/ (m-n) \right\}^{1/2}, \quad w = 1 \Big/ \sigma^2 \left(F_{obs.} \right),$$ m is the number of reflections used, n the number of parameters.

Crystal Structure Determination: A crystal plate was cut out of a larger aggregate and selected after optical examination under crossed polars. The single-crystal X-ray diffraction experiment was performed at r.t. with an Oxford diffraction Xcalibur diffractometer equipped with a CCD detector. A full redundant Ewald sphere was collected with Mo(K_α) radiation up to a maximum resolution $sin\theta/\lambda max = 0.88$ Å^{-1}. Bragg intensities were integrated with Crysalis software,[33] and averaged in Laue point group mmm with SORTAV program[34] after an absorption correction ($\mu = 4.45$ mm^{-1}) based on the crystal shape. Data collection details are summarized in Table 4. The crystal structure was solved by direct methods using SHELXS[35] and refined with JANA2000.[36] The positions of all non-hydrogen atoms were found straightforwardly on successive Fourier maps. Hydrogen atoms were introduced in the structural model by assuming ideal conformations for all ethylamine molecules. Atomic displacement parameters of H atoms were restrained to 1.5 times the value of that of the heavy atom they were attached to. All bond lengths and bond angles of ethylamine molecules were also restrained to the expected values observed in CH_3 (methyl), CH_2 (methylene), and NH_3 (amine) groups.[37] The refinement converged to $R = 0.054$ and $R_W = 0.058$ for the 4642 observed reflections [$I > 3\sigma(I)$]. Selected bond lengths are given in Table 5. CCDC-645100 contains the supplementary crystallographic data for this paper. These data can be obtained free of charge from The Cambridge Crystallographic Data Centre via www.ccdc.cam.ac.uk/data_request/cif.

Table 5. Selected bond lengths [Å] in the fluorogallophosphate Mu-35.

Bond	Length [Å]	Bond	Length [Å]	Bond	Length [Å]
Ga1–O1	1.911(4)	Ga2–O5	1.826(4)	Ga3–O9	1.837(4)
Ga1–O3	1.924(4)	Ga2–O7	1.846(4)	Ga3–O10	1.860(4)
Ga1–O2	1.929(4)	Ga2–O6	1.849(4)	Ga3–O11	1.866(4)
Ga1–O4	1.933(4)	Ga2–O8	1.943(4)		
Ga1–F1	1.977(3)	Ga2–F1	2.025(3)	Ga3–F2	2.009(3)
Ga1–F2	1.981(3)				
			apical F	Ga3–F3	1.864(4)
P1–O5	1.524(4)	P2–O3	1.521(4)	P3–O4	1.517(4)
P1–O2	1.532(4)	P2–O1	1.526(4)	P3–O11	1.537(4)
P1–O8	1.534(4)	P2–O7	1.530(4)	P3–O6	1.540(4)
P1–O9	1.538(4)	P2–O10	1.544(4)		
			apical O	P3–O12	1.533(4)

Supporting Information (see footnote on the first page of this article): Atomic coordinates and displacement parameters at the end of structural refinement as well as selected angles. Projection of the structure of the fluorogallophosphate Mu-35 along the *c* axis in color.

[1] M. E. Davis, *Nature* **2002**, *417*, 813.
[2] S. T. Wilson, B. M. Lok, C. A. Messina, T. R. Cannan, E. M. Flanigen, *J. Am. Chem. Soc.* **1982**, *104*, 1146.
[3] H. Kessler, J. Patarin, C. Schott-Darie, "Advanced Zeolite Science and Applications" in *Studies in Surface Science and Catalysis* (Eds.: J. C. Jansen, M. Stöcker, H. G. Karge, J. Weitkamp), Elsevier, Amsterdam, **1994**, vol. 85, p. 75.
[4] G. Férey, *J. Fluorine Chem.* **1995**, *72*, 187.
[5] J. Patarin, J. L. Paillaud, H. Kessler in *Synthesis of AlPO4s and Other Crystalline Materials, Handbook of Porous Solids* (Eds.: F. Schüth, K. S. Sing, J. Weitkamp), Wiley-VCH, Germany, **2002**, vol. 2, ch. 4.2.3, p. 815.
[6] M. Estermann, L. B. McCusker, Ch. Baerlocher, A. Merrouche, H. Kessler, *Nature* **1991**, *352*, 320.
[7] A. Matijasic, P. Reinert, L. Josien, A. Simon, J. Patarin, "Zeolites and Mesoporous Materials at the Dawn of the 21st Century" in *Studies in Surface Science and Catalysis* (Eds.: A. Galarneau, F. Direnzo, F. Fajula, J. Vedrine), Elsevier, Amsterdam, vol. 135, **2001**, p. 142.
[8] P. Caullet, J. L. Paillaud, A. Simon-Masseron, M. Soulard, J. Patarin, *C. R. Chimie* **2005**, *8*, 245.
[9] L. Vidal, V. Gramlich, J. Patarin, Z. Gabelica, *Eur. J. Solid State Inorg. Chem.* **1998**, *35*, 545.
[10] L. Vidal, V. Gramlich, J. Patarin, Z. Gabelica, *Chem. Lett.* **1999**, 201.
[11] C. Paulet, T. Loiseau, G. Férey, *J. Mater. Chem.* **2000**, *10*, 1225.
[12] L. Lakiss, A. Simon-Masseron, V. Gramlich, J. Patarin, *J. Solid State Sci.* **2005**, *7*, 141.
[13] L. Lakiss, A. Simon-Masseron, J. Patarin, *Microporous Mesoporous Mater.* **2005**, *84*, 50.
[14] C. Marichal, J. M. Chézeau, M. Roux, J. Patarin, J. Luis Jorda, L. B. McCusker, C. Baerlocher, P. Pattison, *Microporous Mesoporous Mater.* **2006**, *90*, 5.
[15] L. Lakiss, A. Simon-Masseron, F. Porcher, J. Patarin, *Eur. J. Inorg. Chem.* **2006**, 237.
[16] A. M. Chippindale, S. Natarajan, J. M. Thomas, R. H. Jones, *J. Solid State Chem.* **1994**, *111*, 18.
[17] T. Loiseau, G. Férey, *Eur. J. Solid State Inorg. Chem.* **1994**, *31*, 575.
[18] T. Loiseau, C. Paulet, N. Simon, V. Munch, F. Taulelle, G. Férey, *Chem. Mater.* **2000**, *12*, 1393.
[19] R. N. Devi, K. Vidyasagar, *J. Chem. Soc. Dalton Trans.* **2000**, *10*, 1605.
[20] J. N. Behera, C. N. R. Rao, *J. Am. Chem. Soc.* **2006**, *128*, 9334.
[21] S. J. Weigel, R. E. Morris, G. D. Stucky, A. K. Cheetham, *J. Mater. Chem.* **1998**, *8*, 1607.
[22] E. R. Cooper, C. D. Andrews, P. S. Wheatley, P. B. Webb, P. Wormald, R. E. Morris, *Nature* **2004**, *430*, 1012.
[23] E. R. Parnham, E. A. Drylie, P. S. Wheatley, A. M. Z. Slawin, R. E. Morris, *Angew. Chem.* **2006**, *118*, 5084.
[24] S. Feng, R. Xu, *Chem. J. Chinese Univ.* **1988**, *4*, 1.
[25] F. Serpaggi, T. Loiseau, D. Riou, G. Férey, M. W. Hosseini, *Eur. J. Solid State Inorg. Chem.* **1994**, *31*, 595.
[26] L. Beitone, J. Marrot, T. Loiseau, G. Férey, M. Henry, C. Huguenard, A. Gansmuller, F. Taulelle, *J. Am. Chem. Soc.* **2003**, *125*, 1912.
[27] H. O. Kalinowski, S. Berger, S. Braun, *^{13}C NMR Spektroskopie*, Georg Thieme, Stuttgart, New York, **1984**, p. 189.
[28] A. Matijasic, V. Gramlich, J. Patarin, *J. Solid State Sci.* **2001**, *3*, 155.
[29] A. Matijasic, V. Gramlich, J. Patarin, *J. Mater. Chem.* **2001**, *11*, 2553.
[30] L. Josien, A. Simon-Masseron, V. Gramlich, J. Patarin, *Chem. Eur. J.* **2002**, *8*, 1614.
[31] C. Schott-Darie, PhD Thesis, University of Haute Alsace, Mulhouse, **1994**.
[32] http://crmht-europe.cnrs-orleans.fr/dmfit/, D. Massiot, F. Fayon, M. Capron, I. King, S. Le Calvé, B. Alonso, J. O. Durand, B. Bujoli, Z. Gan, G. Hoatson, *Magn. Reson. Chem.* **2002**, *40*, 70.
[33] *Crysalis Software system*, Version 1.170, Oxford Diffraction Ltd, **2003**.
[34] R. H. Blessing, *J. Appl. Crystallogr.* **1997**, *30*, 421.
[35] G. M. Sheldrick, *SHELXS86: Program for the Solution of Crystal Structures*, Institut für Anorganische Chemie der Universität, Göttingen, Germany, **1986**.
[36] V. Petříček, M. Dušek, *The Crystallographic Computing System JANA2000*, Institute of Physics, Praha, Czech Republic, **2000**.
[37] *International Tables for X-ray Crystallography – Vol. C*. Kluwer Academic Publishers, Dordrecht.

Received: March 5, 2007
Published Online: July 11, 2007

